

Leukocyte spreading behavior on vascular biomaterial surfaces: consequences of chemoattractant stimulation

Charlie C. Chang, Scott M. Lieberman, Prabhas V. Moghe*

Department of Chemical and Biochemical Engineering, Rutgers University, Busch Campus, 98 Brett Road, Piscataway, NJ 08854-8058, USA

Received 20 April 1998; accepted 10 July 1998

Abstract

Chemoattractant-induced phenomena of polarity and migration of polymorphonuclear leukocytes (PMN) are believed to play a key physiological role in controlling bacterial infections on implantable vascular biomaterials. Our study targeted the spreading behavior of human PMN adherent to expanded polytetrafluoroethylene (ePTFE), pretreated with various plasma proteins, in response to the chemoattractant, *N*-formyl-methionyl-leucyl-phenylalanine (fMLP). To this end, a novel imaging configuration was developed to allow in situ reconstructive analysis of PMN 3-D morphology on opaque ePTFE surfaces, using optical sectioning confocal microscopy. Following fMLP stimulation, PMN morphological polarity was enhanced on all substrates studied except fibrinogen treated ePTFE. 3-D PMN morphometry revealed that in the absence of fMLP, overall cell spreading was minimized on albumin-treated ePTFE and maximized on fibrinogen and immunoglobulin-G-treated ePTFE. Following fMLP stimulation, overall PMN spreading increased markedly on untreated and albumin-coated ePTFE, while it stayed invariant on IgG and plasma treated ePTFE, and decreased on fibrinogen-treated ePTFE. Spatial analysis of PMN spreading following fMLP stimulation revealed enhanced PMN attachment on untreated and albumin treated ePTFE and diminished attachment on fibrinogen and plasma treated ePTFE. Thus, chemoattractant stimulation altered a wide range of PMN spreading attributes on ePTFE, including morphological polarity, substrate attachment, and 3-D membrane spreading, in a substrate dependent manner. These chemoattractant-induced spreading responses may also have important consequences for PMN phagocytosis. We report that fMLP stimulation led to enhanced unopsonized particulate phagocytosis on untreated and albumin treated ePTFE, but caused no discernible change in phagocytosis on other protein substrates. Thus, chemoattractant modulation of PMN spreading on ePTFE is highly substrate-regulated, and manifests in concerted effects on PMN phagocytosis. © 1999 Elsevier Science Ltd. All rights reserved

Keywords: Chemoattractant; Vascular biomaterials

1. Introduction

A problem recurrent with artificial implantable biomaterials, particularly those constituting vascular grafts, is periprosthetic bacterial infections [1]. Infected synthetic vascular grafts exhibit steady colonization of graft interstices by bacteria, a process that is initiated early on, and can continue over long periods of time [2]. Patient mortality rates due to infected grafts may range from 25 to 75%, and complications of multiple operative procedures and hospitalization frequently cause extended

morbidity [3]. Several early reports [3–5] and more recent updates [1, 6] have documented the clinical manifestation and management of graft infections.

Polymorphonuclear leukocytes (PMN, or neutrophils), the predominant migratory phagocytic cells of circulating blood, are the first cells to arrive at sites of infection, and are crucial effectors of host defense against bacterial infections. PMN carry out this activity by migrating into extravascular regions of infection under the influence of locally released soluble factors, called chemoattractants [7] and then ingesting, or phagocytosing bacteria [8]. A similar pattern of phagocytic activity to that evoked by bacteria is observed in their absence when PMN come in contact with synthetic biomaterial surfaces, a process termed ‘frustrated phagocytosis’ as the cell unsuccessfully attempts to surround the biomaterial

*Corresponding author. Tel.: 001 732 445 4951; fax: 001 732 445 2581; e-mail: moghe@rci.rutgers.edu

[9]. Thus, the degree of PMN spreading on vascular biomaterial surface reflects sensitively the ensuing cell–biomaterial interactions as well as the attendant PMN activation events. Abnormal levels of leukocyte spreading have been shown to severely limit particulate phagocytosis [10]. Given previous correlations between PMN shape, polarity (asymmetry) and migratory potential [11, 12], it is likely that the morphological changes of biomaterial-adherent PMN may be indicative of their migratory functions as well. While PMN spreading phenomena on vascular biomaterials are recognized to be important, it is not clear how they are modulated by the process of chemoattractant stimulation which acts as the ubiquitous cue for PMN polarization and migration. This information would be vital to effect physiological changes in PMN–biomaterial interactions, particularly in the vicinity of chemoattractant-releasing bacteria and during stages of acute inflammation [7].

The interaction between circulating PMN and implanted vascular biomaterial surfaces is further affected by the surface layer of host proteins acquired instantly after implantation [13]. Of the 150 or so proteins of blood plasma [14], the most abundant components including albumin, fibrinogen, and immunoglobulin [15, 16] can elicit very distinct cellular interactions. Preadsorbed albumin (HSA) can passivate surfaces [17–19] while adsorbed IgG can activate complement, which in turn induces PMN attachment to the surface [20] and activates PMN phagocytic functions [21]. Fibrinogen, a key molecule in acute inflammatory responses to implanted polymers [22] induces leukocytes to exhibit rapid spreading [23, 24]. It is not clear however how leukocyte spreading may be modulated on protein-preadsorbed biomaterial surfaces in the extended presence of chemoattractants. These insights would be particularly useful to assess the extent of biomaterial surface involvement in regulating leukocyte function and ultimately controlling bacterial infections.

In this paper, we have investigated the effect of chemical stimulation by the chemotactic peptide, *N*-formyl-methionyl-leucyl-phenylalanine (fMLP), on the spreading behavior of human polymorphonuclear leukocytes (PMN) adherent to expanded polytetrafluoroethylene (ePTFE). To this end, the extent of leukocyte spreading behavior was characterized comprehensively in terms of a 3-D shape factor and its volume distribution. Unlike traditional 2-D imaging approaches, 3-D morphometry captures both core cell shape changes as well as any protrusive activity of the cell membrane. From our analysis, we report that 3-D morphological parameters of PMN is strongly dependent on the nature of ePTFE pretreatment, and are differentially modulated by chemoattractant exposure. To further investigate how fMLP-induced intrinsic shape changes may effect PMN bactericidal activities, we quantified the resultant PMN

uptake of non-opsonized bacteria, that is, in the absence of any immunological mediation. Following fMLP stimulation, substrates that elicited morphological polarization and spreading of PMN in limit also caused enhanced particulate phagocytosis.

2. Materials and methods

2.1. Biomaterial and reagents

Expanded polytetrafluoroethylene (ePTFE) was generously donated by W.L. Gore and Associates, Inc. (Flagstaff, AZ). Ninety-six-well flat bottomed plates (Falcon, 3933) were obtained from Becton Dickinson Co. (Lincoln Park, NJ). PMN isolation medium and erythrocyte lysis buffer (E-LYSE) were obtained from Cardinal Associates (Santa Fe, New Mexico). Human serum albumin (HSA), fibrinogen, dimethyl sulfoxide (DMSO), phorbol 12-myristate 13-acetate (PMA) and formyl-methionyl-leucyl-phenylalanine (fMLP) were obtained from Sigma Chemical Co. (St. Louis, MO). CellTracker™ CM-DiI (DiI: C7000) was obtained from Molecular Probes (Eugene, OR). Hanks' balanced salt solution (HBSS) and HBSS without calcium and magnesium were obtained from Gibco BRL Life Technologies, Inc. (Grand Island, NY).

2.2. Plate preparation

Adhesion and phagocytosis assays were conducted in 96-well plates. Gas sterilized, regular thickness, ePTFE discs with 30 μm internodal spacing were placed at the bottom of wells and held in place with polystyrene rings as previously described [19]. The ePTFE discs and wells were rinsed three times with 200 μl of HBSS each washing. For plasma coating, the ePTFE discs were incubated for 3 h at 37°C with 200 μl well⁻¹ platelet poor human plasma solution. For HSA coating, the ePTFE discs were incubated for 3 h at 37°C with 200 μl well⁻¹ of 5% HSA solution. For fibrinogen coating, the ePTFE discs were incubated for 3 h at 37°C with 200 μl well⁻¹ of fibrinogen solution at a concentration of 1 mg ml⁻¹. All wells were washed thrice with HBSS (200 μl well wash⁻¹) at 37°C using a manual multichannel pipette before adding PMN. The concentration of all proteins used for ePTFE treatment was based on the physiological concentration of the proteins in plasma [14].

2.3. PMN isolation

Twenty ml of blood was drawn from healthy volunteer donors in accordance with the protocols established by the Rutgers University Institutional Review Board. PMN were isolated by the single-step density gradient centrifugation using a modification of Boyum's tech-

nique [25]. Briefly, the blood was layered on top of half its volume of ficoll hypaque and centrifuged at 1380 rpm for 30 min at room temperature. The PMN-rich layer was aspirated, washed, and centrifuged with HBSS without calcium and magnesium. In order to sediment the red blood cells, the PMN pellet was then diluted in 3 ml E-lyse and resuspended in HBSS at a concentration of 2×10^6 cells ml⁻¹ and incubated at 4°C. PMN preparations were greater than 97% viable as determined by trypan blue exclusion.

2.4. Cell labeling

CellTracker™ CM-DiI, a derivative of DiIC₁₈, was used to fluorescently label PMN membranes. DiI molecules excite and emit at 553 and 570 nm, respectively. A stock solution of 50 µg of DiI was diluted with 50 µl of DMSO and stored at -20°C. For cell labeling, this solution was diluted to 2 µM in HBSS containing approximately 10×10^6 PMN. The solution was incubated first at 37°C for 5 min and then at 4°C for 10 min. After washing with 10 ml of HBSS and centrifuging at 1000 rpm for 10 min, the PMN solution was then resuspended at 2×10^6 cells ml⁻¹ of HBSS.

2.5. Cell spreading assay

Pre-DiI labeled PMN at 2×10^5 cells 200 µl well⁻¹ were added to 96-well plates and incubated with protein pretreated ePTFE discs for 30 min at 37°C. A portion of the PMN suspension was exposed to fMLP (10^{-8} M) immediately prior to the incubation. Non-adherent cells were then removed and the wells with biomaterial were rinsed thrice with warm HBSS (200 µl well⁻¹ wash⁻¹). Two percent glutaraldehyde in phosphate buffer solution (0.05 M) was immediately added to the wells with biomaterial to fix the adhered PMN. After 30 min of incubation at room temperature, the biomaterials were rinsed in phosphate buffer saline thrice (200 µl well⁻¹ wash⁻¹). The specimens were then placed on MatTek chambers (MatTek Corporation, Ashland, MA) and examined using confocal microscopy.

2.6. Confocal imaging

Confocal laser-scanning microscopy (CLSM) was conducted on a Zeiss LSM 410 workstation (Zeiss Inc., Thornwood, NY). Specimens were excited at 488 nm, and images at 520 nm emission were obtained at a magnification of 100× and a zoom of 5× using a 510 nm long pass filter. Thirteen to twenty-five optical sections were obtained at 0.5 µm increments in depth for each specimen. The confocal images were then processed and analyzed using KS400 image analysis software (Kontron Elektronik, Germany).

2.7. Image analysis

2.7.1. 2-D PMN polarity

The original confocal images were first binarized using the ‘thresholding’ function, in which each segmented pixel was assigned to either black or white. The binary images were then filtered to eliminate the intensity spikes that may appear in the filter mask and regions of low grey value within cellular boundaries were rendered contiguous via ‘filling’. Finally, the following geometric features were determined for each object element: (i) area of the region; (ii) perimeter of the convex hull of the region; and (iii) lengths of the primary and secondary axes of the ellipse with the same center of gravity. Using the section of each cell corresponding to the highest area, the 2-D polarity factor was computed. The 2-D polarity factor was defined as the ratio of the lengths of major to minor axes of an ellipse having the same center of gravity as the PMN. A circular object would have a polarity factor of unity.

2.7.2. 3-D PMN spreading

To provide a more complete quantification of the cell morphological topology, we formulated a 3-D shape factor (ϕ_{3D}) which was defined to be

$$\phi_{3D} = \frac{(\text{Surface Area})^3}{36\pi(\text{Volume})^2}$$

Rather than being derived from a single section, the 3-D shape factor thus was computed by optically sectioning each ePTFE-adherent PMN from top to bottom and reconstructing the entire cell volume and cell surface area. Values of perimeter and area were computed for all optical sections. Since the incremental distance between neighboring optical sections was sufficiently small (0.5 µm), using a trapezoidal approximation, the volume of the cell was computed as the integrated product of the average area of every two adjacent sections and the intervening thickness, across the scanned depth of each cell. Cell surface area was estimated in a similar manner using the values of the section perimeter instead of the area. A spherical object would have a 3-D shape factor of unity and non-spherical object would have a 3-D shape factor greater than unity, suggestive of increased 3-D spreading. In this study, the polarity factor and shape factor of PMN were normalized to the respective values for unstimulated PMN on albumin treated ePTFE (control).

2.8. Phagocytosis assay

One milliliter of pre-labeled fluorescent E. coli bioparticle solution (Molecular Probes, OR) was washed three times with 10 ml wash⁻¹ of HBSS. The bioparticle pellet was then resuspended in 3 ml of HBSS and sonicated for

30 s at a setting of 2 using the Sonic Dismembrator 60 (Fisher, NJ). 200 μl of bioparticle solution/well was added to PMN spread on ePTFE precoated with different proteins as described previously. The plate was then incubated for 1 h at 37°C. Following incubation, the cells were fixed with 200 μl well⁻¹ of 2% glutaraldehyde in PBS. The ePTFE discs were placed in MatTek chambers and observed under fluorescence microscopy. The number of phagocytosed *E. coli* particles was quantified and divided by a total of two hundred cells per condition.

2.9. Statistical analysis

Thirteen to twenty-five optical sections of 0.5 μm thickness were analyzed for 12 cells within each condition, and the ratio of major to minor axes, perimeter, and area were determined for each section. Statistical analyses were performed using unpaired *t*-test and ANOVA, and a confidence level of 95% ($P < 0.05$) was considered necessary for statistical significance. The error bars indicate the standard error around the mean value.

3. Results

3.1. Qualitative analysis of PMN morphology

PMN morphology on uncoated, HSA, fibrinogen, IgG and plasma coated ePTFE was examined qualitatively using confocal microscopy. On uncoated ePTFE surfaces, PMN spreading was polarized and exhibited a dominant lamellipodium (Fig. 1a). In contrast, on albumin and serum coated biomaterial surfaces, PMN were found

to be more or less rounded with no discernible polarity (Fig. 1b and c). On fibrinogen- and IgG-coated biomaterial, PMN appeared randomly spread and weakly polarized (Fig. 1d, e).

The incubation of PMN with fMLP evoked a distinct change in cell morphology. Stimulated PMN on uncoated ePTFE exhibited increased morphological asymmetry (Fig. 1f). On albumin coated ePTFE, fMLP stimulated PMN showed enhanced polarity as well as spreading (Fig. 1g). In contrast, fMLP-stimulation on fibrinogen treated ePTFE caused a retraction of cell ruffles and overall cell compaction (Fig. 1h). Finally, on IgG- and plasma-coated biomaterial, fMLP stimulation caused a marked elongation in cell shape (Fig. 1i and j).

3.2. 2-D quantitation of PMN polarity

The 2-D polarity factor quantifies the asymmetry of PMN spreading. As shown in Fig. 2, unstimulated PMN on untreated ePTFE were the most polarized (1.34 ± 0.08), while PMN on the albumin coated ePTFE showed the least polarization (1.00 ± 0.02). Stimulation with fMLP caused a statistically significant increase in the degree of PMN polarity on untreated ePTFE (1.68 ± 0.16) and on ePTFE treated with albumin (1.33 ± 0.11), IgG (1.61 ± 0.04) or plasma (1.23 ± 0.04). However, on fibrinogen coated ePTFE no significant changes in PMN polarity were observed (1.17 ± 0.03).

3.3. 3-D quantitation of PMN spreading

A spatially integrated shape factor (ϕ_{3D}) was computed to determine the 3-D extent of PMN spreading on the

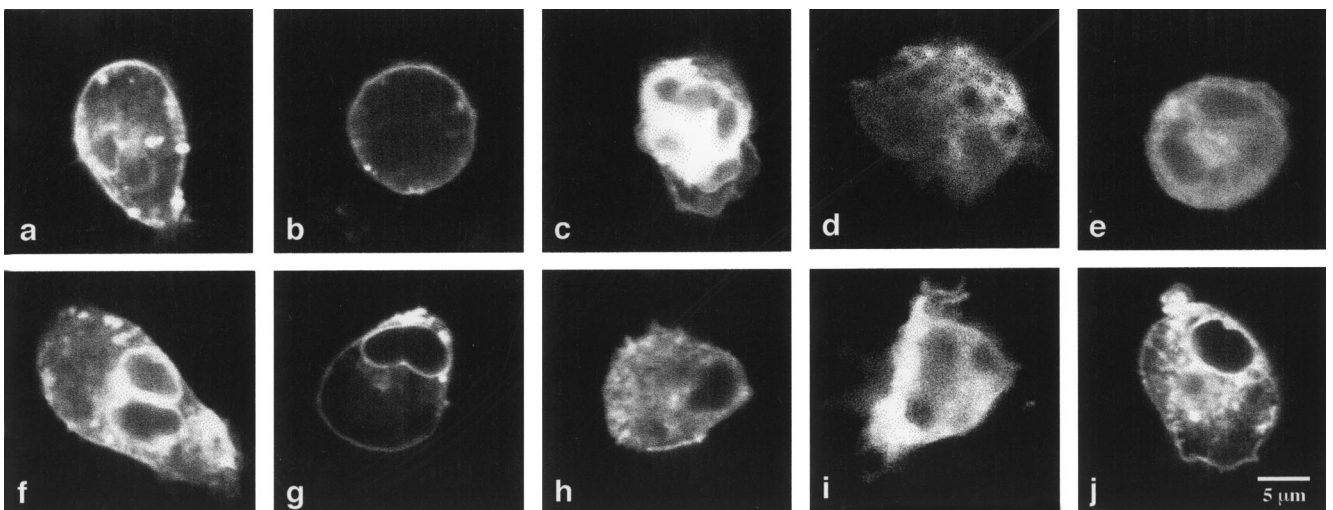


Fig. 1. Confocal micrographs of the spreading behavior of unstimulated fluorescently labeled PMN were obtained on ePTFE surfaces pretreated with (a) HBSS, (b) albumin, (c) fibrinogen, (d) IgG, and (e) plasma. Confocal micrographs of the spreading behavior of fMLP-stimulated fluorescently labeled PMN were obtained on ePTFE surfaces pretreated with (f) HBSS, (g) albumin, (h) fibrinogen, (i) IgG, and (j) plasma. PMN were incubated on all biomaterial surfaces for 30 min prior to fixation and imaging.

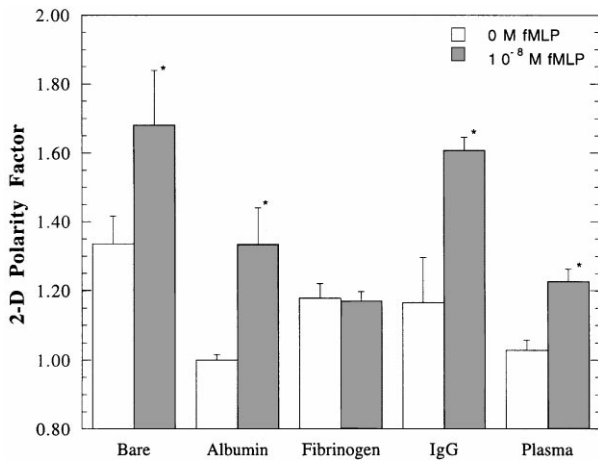


Fig. 2. Degree of polarization of PMN after 30 min incubation on ePTFE surfaces was quantitated ($n = 15$ cells) in terms of 2-D polarity factor and normalized to that observed on albumin. Various conditions include: (a) uncoated ePTFE, (b) albumin-coated ePTFE, (c) fibrinogen-coated ePTFE, (d) IgG-coated ePTFE and (e) plasma-coated ePTFE. *: $P < 0.05$.

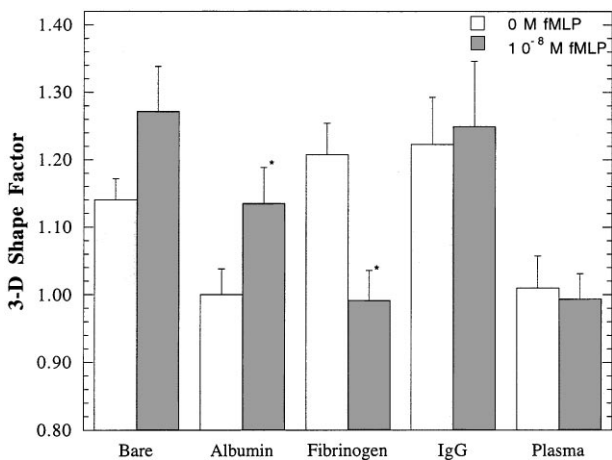


Fig. 3. Degree of spreading of PMN on ePTFE surfaces was quantitated in terms of 3-D shape factor and normalized to that observed for unstimulated PMN on albumin. Various conditions include: (a) uncoated ePTFE, (b) albumin-coated ePTFE, (c) fibrinogen-coated ePTFE, (d) IgG-coated ePTFE and (e) plasma-coated ePTFE. *: $P < 0.05$.

ePTFE. As shown in Fig. 3, unstimulated PMN on uncoated ePTFE (1.14 ± 0.03) and on ePTFE treated with fibrinogen (1.21 ± 0.05) or IgG (1.22 ± 0.07) have a notably higher shape factor compared to those on ePTFE treated with albumin (1.00 ± 0.04) and plasma (1.01 ± 0.05). Upon the addition of fMLP, PMN on the untreated ePTFE (1.27 ± 0.07) and albumin treated ePTFE (1.13 ± 0.05) exhibited increased 3-D shape factor. Intriguingly, following fMLP stimulation, the 3-D shape factor was decreased on fibrinogen treated ePTFE (0.99 ± 0.04), while no significant difference was detected

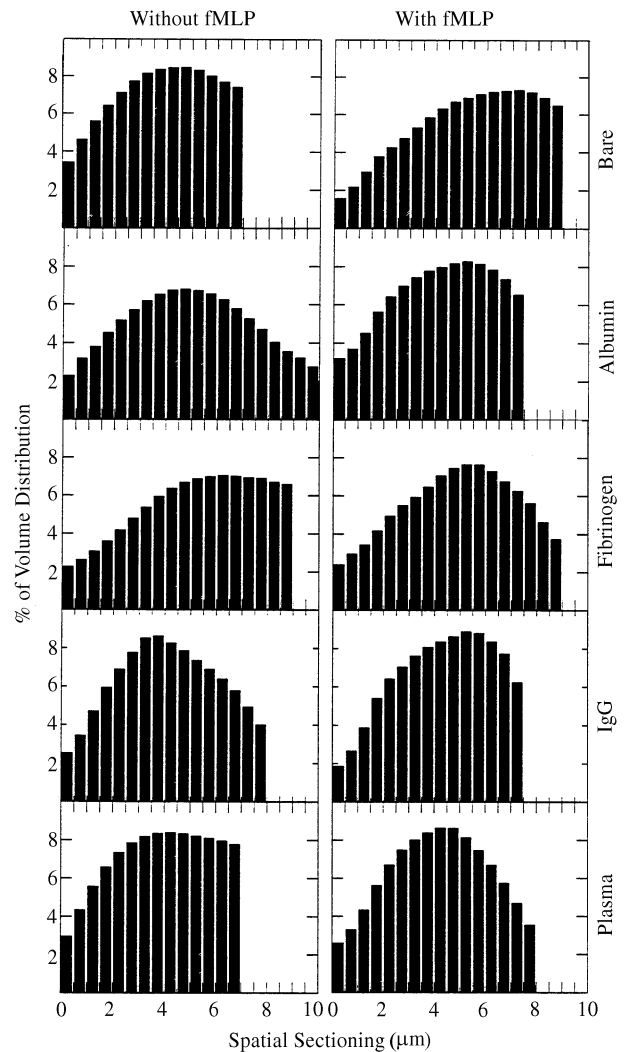


Fig. 4. Spatial volume distribution of PMN was computed with and without fMLP stimulation on ePTFE surfaces pretreated with HBSS, albumin, fibrinogen, IgG and plasma. The volume fraction was plotted for various optical sections, from top of the cell (prescribed to be $z = 0 \mu\text{m}$) to bottom of the cell in contact with the biomaterial surface.

in ϕ_{3D} of PMN on ePTFE treated with IgG (1.25 ± 0.10) or plasma (0.99 ± 0.04).

3.4. Spatial distribution of PMN volume

The spatial distribution of PMN volume, $V(z)$, was computed to quantify the extent of substrate-based PMN attachment. The panel of graphs in Fig. 4 depicts PMN volume fraction corresponding to every incremental optical section starting from the top of the cell to the bottom of the cell body that is in contact with ePTFE. On albumin coated ePTFE, $V(z)$ for unstimulated PMN was more or less symmetric (mean skewness, $\langle S \rangle = 0.49$) with a small area of contact with ePTFE (Fig. 5b). Stimulation with fMLP caused a pronounced shift in $V(z)$ toward regions of biomaterial contact ($\langle S \rangle = 0.93$). On

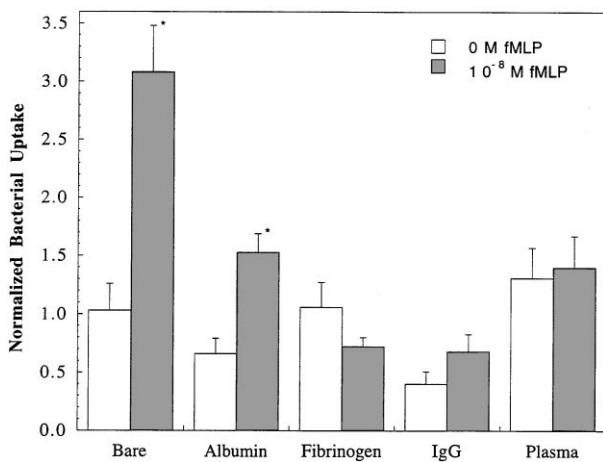


Fig. 5. The phagocytic capacity of activated PMN was quantified on ePTFE surfaces pretreated with various plasma proteins and in the presence of fMLP stimulation.

fibrinogen coated surfaces, in contrast, $V(z)$ was skewed toward the biomaterial contact ($\langle S \rangle = 0.82$) for unstimulated PMN, indicating increased membrane spreading on ePTFE while fMLP stimulation caused a decrease in $V(z)$ levels proximal to the biomaterial contact. $V(z)$ for sections at the distal end from the PMN-biomaterial contact did not change significantly however, and the overall skewness of $V(z)$ declined slightly ($\langle S \rangle = 0.76$). $V(z)$ responses on fibrinogen-treated ePTFE were similar to those observed on plasma pretreated ePTFE. Upon fMLP stimulation, the symmetric PMN volume distribution on IgG treated ePTFE ($\langle S \rangle = 0.57$) became significantly skewed toward biomaterial interface ($\langle S \rangle = 1.1$).

3.5. Particulate phagocytosis

Only slight variations in PMN bacterial uptake levels were seen in the absence of fMLP on all pretreated substrates. Upon stimulation with fMLP, however, a striking increase in bacterial uptake levels was observed on bare ePTFE and on albumin treated ePTFE. No significant changes in the levels of bacterial uptake were found under any other conditions examined (Fig. 5).

4. Discussion

In this study, we have examined the spreading and polarization behavior of PMN on an opaque vascular biomaterial using in situ imaging and reconstruction analysis. Cell spreading on opaque biomaterials has been conventionally studied using techniques such as scanning electron microscopy (SEM); however, SEM data do not lend themselves to quantitative three-dimensional mor-

phometry. Instead, we have employed confocal fluorescence microscopy in conjunction with 3-D reconstructive optical sectioning to spatially quantitate PMN spreading. The resultant three-dimensional data provide computation of the core cell shape changes, protrusive activity of cell membrane, and interfacial PMN coverage on the biomaterial, features that are not deduced by 2-D measurements.

Our studies were designed to discern PMN spreading responses to exogenous effects of a soluble stimulator (fMLP) relative to PMN spreading responses to untreated and protein-adsorbed ePTFE. Even unmodified ePTFE surface by itself was sufficient to trigger enhanced PMN spreading as confirmed quantitatively by the high 2-D polarity and 3-D shape factor. Pretreatment with various plasma proteins further altered this spreading behavior with a high degree of protein specificity. Previous studies show that plasma proteins do not cause polarization of cells in suspension [26]. Our morphometric studies revealed that specific protein pretreatment of the substrate can indeed result in *differential* changes in 2-D polarity, membrane spreading, as well as core cell shape. For instance, trends of unisectonal 2-D polarity indicated that the PMN on ePTFE pretreated with albumin and plasma were rounded, typical of unactivated PMN [17–19]. However, 3-D studies of the spatial evolution of PMN shape showed that the volume distribution of PMN on these substrates, in fact, diverged substantially. In the absence of exogenous stimulation, 2-D polarity and spatially integrated 3-D spreading (shape factor) demonstrated several substrate-based differences. For example, while unstimulated PMN on every protein-treated substrate showed comparable, low levels of 2-D polarity, PMN 3-D spreading behavior varied significantly, particularly on fibrinogen and IgG substrates, where spreading was greatly augmented compared to other treated substrates. This excessive spreading has parallels to ‘frustrated spreading’, commonly associated with increased PMN adhesiveness and compromised polarity [27, 28].

Chemotactic stimulation of PMN has been shown to promote membrane ruffling [29] and to generally cause increased PMN attachment to the substrate [17]. Our studies indicate that fMLP stimulation elicited cellular spreading that was highly regulated by the nature of the substrate. For instance, while cell spreading was enhanced on uncoated ePTFE and albumin treated ePTFE, it was diminished on fibrinogen coated ePTFE and minimally altered on IgG and plasma treated ePTFE. The mechanistic causes underlying these substrate specific differences in cell spreading are presently unclear, although receptor–substrate interactions are expected to play a major role. For instance, candidate molecules such as leukocyte β_2 integrins are thought to likely mediate PMN adhesion to vascular prosthetic materials [30]. On albumin-treated ePTFE, PMN adhesion

is primarily mediated via CD43, an anti-spreading PMN receptor, that arrests PMN polarization and spreading [18]. The effect of CD43 has also been reported to be reversed by the addition of a chemoattractant [18], consistent with our findings that PMN contraction is reversed on albumin following fMLP stimulation. On fibrinogen-treated ePTFE, PMN adhesion is likely regulated by CD11b/CD18, a member of leukocyte integrin family [31–34], as well as the highly conserved 95-kDA β chain of the integrin family [35]. Our results showed that fMLP stimulation led to retraction of cell spreading on fibrinogen and simultaneous reduction of overall cell polarity, thereby yielding increased 3-D shape factor and greater depth symmetry of PMN volume distribution. Previously, fibrinogen has been shown to counteract the effect of fMLP-like secretagogues on PMN activities such as adhesion [36] and chemotactic migration [37, 38], presumably via interactions between PMN β_1 integrins and fibrinogen-associated ligands, ultimately causing PMN to become sessile [37, 38]. On IgG, the key PMN receptors that bind to the Fc portion of IgG, Fc γ RII and Fc γ RIII [39, 40], stimulate opsonin-dependent phagocytosis and activate the production of reactive oxygen species (ROS) [21]. These processes may manifest in hyperspreading on IgG such as that observed in our studies. Lastly, the spreading behavior on plasma-treated ePTFE is expected to be orchestrated by the most abundant and stable of the adsorbed components. While the plasma-induced response is complex and difficult to discern systematically, the similarity of PMN volume distribution on fibrinogen and plasma is intriguing, given higher retention levels of fibrinogen documented [41].

We have also investigated the role of PMN spreading on ePTFE in relation to PMN phagocytosis via opsonin-independent mechanisms. These uptake pathways are operative in the absence of complement and immunoglobulin, and are mediated by oligosaccharide-containing moieties on the surface of bacteria and non-immunological receptors on PMN surface [42]. Given their nonimmunological basis, these functional endpoints may be indicative of the intrinsic effects of PMN spreading on vascular biomaterials, and as such, may even provide insights into the early PMN responses to implant-related bacterial infections, prior to antibody-dominated interactions. Previous studies suggest that frustrated spreading and opsonized particulate phagocytosis may be limited in similar ways, but are different from cell spreading on unopsonized surfaces [10]. In our studies, we observed that PMN hyperspreading on opsonizable surfaces such as immunoglobulin-coated ePTFE limits opsonin-independent particulate phagocytosis, both in the absence and presence of fMLP. However, on other, non-opsonizable surfaces, the most significant enhancement in phagocytosis was observed for those conditions (i.e. bare ePTFE and

albumin-treated ePTFE) that also elicited pronounced induction of morphological polarity and membrane spreading. Previously, cytoskeletally mediated shape changes accompanying activation have been shown to respond sensitively to the presence of fMLP in a substrate-specific manner [43, 44]. On IgG, fMLP similarly appears to induce cytoskeletal reorganization that may underlie elevated PMN polarity reported in our studies (data not shown), yet, intriguingly, enhancement in PMN membrane spreading and phagocytosis seems to be limited. This limit is likely posed by saturating levels of either cell surface membrane available for spreading [10] or Fc-receptors required for opsonin-dependent phagocytosis [45], or may be due to surface events accompanying activation and ROS generation [21]. Interestingly, on fibrinogen-coated ePTFE, PMN were also observed to be spread considerably, but phagocytic capability was still low. This may be attributed to the weak ability of fibrinogen to directly activate PMN respiratory burst [21]. Following fMLP stimulation, phagocytic uptake decreased further, albeit insignificantly, which is consistent with the repressed stimulation of fibrinogen by fMLP.

Overall our observations on spreading and phagocytosis behavior reveal substrate-specific parallels to previous reports, where fMLP stimulation of migratory PMN led to increased uptake of unopsonized bacteria but not of Fc-receptor-mediated opsonized bacteria [46]. A pictorial model unifying the plausible substrate and stimulation-dependent pathways is shown in Fig. 6. On substrates such as albumin and bare ePTFE, fMLP stimulation causes preferential release of secondary granule contents [47] and incorporation of their associated membranes into the plasma membrane [48], thus enriching non-immunological receptors, such as fMLP receptors, leading to increased polarity and membrane spreading. On others (e.g. fibrinogen), fMLP interactions with other substrate-related receptors suppress polarity, and membrane incorporation is diminished. On opsonizing substrates such as IgG, while fMLP causes increased polarity, Fc-receptor mediated activation leads to abnormal spreading, and membrane or receptor limitations may ensue. On complex substrates like plasma, the most abundant components or stable conformations may determine the overall response (not shown).

In summary, ePTFE pretreatment that elicited increased membrane spreading, within saturation levels, and enhanced morphological polarity, presumably without significant superoxide activation [21], resulted in improved phagocytic uptake. This understanding provides insights into the basic nature of PMN spreading activities and their possible role, distinct from the effect of opsonin-dependent immunological pathways, in predisposing vascular biomaterials to bacterial infections.

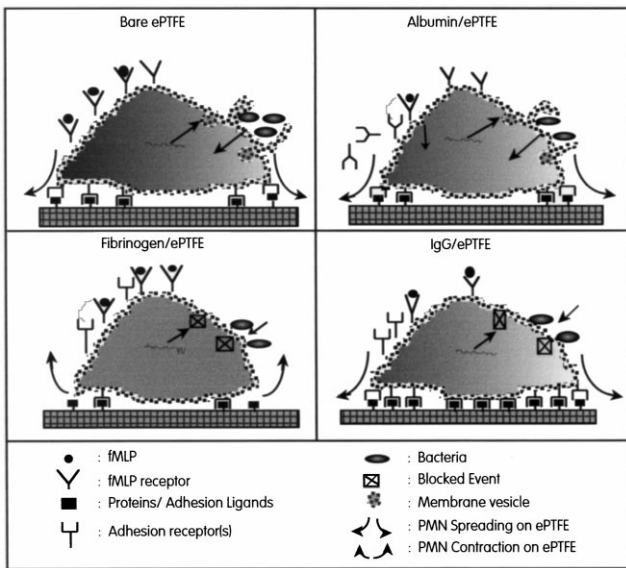


Fig. 6. A symbolic representation of chemoattractant modulation of PMN spreading behavior on ePTFE. The schematic shows key phenomena that may be regulated on pretreated ePTFE, including membrane incorporation into PMN plasma membrane, enrichment of membrane nonimmunological receptors (e.g. fMLP receptors) and immunological receptors (e.g. Fc receptors), PMN spreading or unspreading, shape polarization, substrate receptor interactions with fMLP, and phagocytic uptake of unopsonized particulates.

Acknowledgements

P.V.M. is indebted to Profs. Beatrice Haimovich and Ralph Greco for inspiring the initiation of this study. This study was supported by a Whitaker Foundation Biomedical Engineering Research Grant, the Charles and Johanna Busch Biomedical Research Award, and the Rutgers Research Council Grant to PVM. C.C. was partially supported by the Rutgers/UMDNJ NIH Biotechnology Training Program and the Biomaterials Excellence Award from the New Jersey Center for Biomaterials and Medical Devices. The generous donation of ePTFE from W.L. Gore and Associates Inc. is sincerely appreciated.

References

- [1] Sugarman B, Young EJ. Infections associated with prosthetic devices: magnitude of the problem. *Infectious Disease Clin North Amer* 1989;3:187–98.
- [2] Bhat DJ, Tellis VA, Kohlberg WI, Driscoll B, Veith FJ. Management of sepsis involving expanded polytetrafluoroethylene grafts for hemodialysis access. *Surgery* 1980;87:445–50.
- [3] Bernhard VM. Management of infected vascular prostheses. *Surg Clin North Amer* 1975;55:1411–7.
- [4] Szilagyi DE, Smith RF, Elliott JP, Vrandecic MP. Infection in arterial reconstruction with synthetic grafts. *Ann Surg* 1972;176:321–33.
- [5] Goldstone J, Moore WS. Infection in vascular prostheses. Clinical manifestations and surgical management. *Amer J Surg* 1974;128:225–33.
- [6] Young EJ, Sugarman B. Infections in prosthetic devices. *Surg Clin North Amer* 1988;68:167–80.
- [7] Miller MD, Krangel MS. Biology and biochemistry of the chemokines: a family of chemotactic and inflammatory cytokines. *Crit Rev Immunol* 1992;12:17–46.
- [8] Lehrer RI, Ganz T, Selsted ME, Barbior BM, Curnutte JT. Neutrophils and host defense. *Ann Int Med* 1988;109:127–42.
- [9] Henson PM. The immunologic release of constituents from neutrophil leukocytes. II. Mechanisms of release during phagocytosis and adherence to nonphagocytosable surfaces. *J Immunol* 1971;107:1547–57.
- [10] Cannon GJ, Swanson JA. The macrophage capacity for phagocytosis. *J Cell Sci* 1992;101:907–13.
- [11] Campoccia D, Hunt JA, Doherty PJ, Zhong SP, Callegaro L, Benedetti L, Williams DF. Human neutrophil chemokinesis and polarization induced by hyaluronic acid derivatives. *Biomater* 1993;14:1135–9.
- [12] Ehrenguber MU, Deranleau DA, Coated TD. Shape oscillations of human neutrophil leukocytes: characterization and relationship to cell motility. *J Exper Biol* 1996;199:741–7.
- [13] Baier RE, Dutton RC. Initial events in interactions of blood with a foreign surface. *J Biomed Mater Res* 1969;3:191–206.
- [14] Andrade JD, Hlady V. Plasma protein adsorption: the big twelve. *Ann New York Acad Sci* 1987;516:158–72.
- [15] Anderson JM, Bonfield TL, Ziats NP. Protein adsorption and cellular adhesion and activation on biomedical polymers. *Int J Artif Org* 1990;13:375–82.
- [16] Pankowsky DA, Ziats NP, Topham NS, Ratnoff OD, Anderson JM. Morphologic characteristics of adsorbed human plasma proteins on vascular grafts and biomaterials. *J Vasc Surg* 1990;11:599–606.
- [17] Smith CW, Hollers JC, Patrick RA, Hassett C. Motility and adhesiveness in human neutrophils. *J Clin Invest* 1979;63:221–9.
- [18] Nathan C, Xie Q, Halbwachs-Mecarelli L, Jin WW. Albumin inhibits neutrophil spreading and hydrogen peroxide release by blocking the shedding of CD43 (sialophorin leukosialin). *J Cell Biol* 1993;122:243–56.
- [19] Katz DA, Haimovich B, Greco RS. Neutrophil activation by expanded polytetrafluoroethylene is dependent on the induction of protein phosphorylation. *Surg* 1994;116:446–55.
- [20] O'Flaherty JT, Kruetzer DL, Ward PA. Chemotactic factor influences on the aggregation swelling and foreign surface adhesiveness of human leukocytes. *Am J Pathol* 1978;90:537.
- [21] Liu L, Elwing H, Karlsson A, Nimer G, Dahlgren C. Surface-related triggering of the neutrophil respiratory burst. Characterization of the response induced by IgG adsorbed to hydrophilic and hydrophobic glass surfaces. *Clin Exp Immunol* 1997;109:204–10.
- [22] Tang L, Eaton J. Fibrinogen mediates acute inflammatory responses. *J Exper Med* 1993;178:2147–56.
- [23] Kvarstein B. Effects of proteins and inorganic ions on the adhesiveness of human leukocytes to glass beads. *Scand J Clin Lab Invest* 1969;24:41–8.
- [24] Loike JD, Sodeik B, Cao L, Leucona S, Weitz JI, Detmers PA, Wright SD, Silverstein SC. CD11c/CD18 on neutrophils recognized a domain at N terminus of the A alpha chain of fibrinogen. *Proc Natl Acad Sci* 1991;88:1044–8.
- [25] Ferrante A, Thong YH. Optimal conditions for simultaneous purification of mononuclear and polymorphonuclear leucocytes from human blood by the Hypaque-Ficoll method. *J Immunol Meth* 1980;36:109–17.
- [26] Bignold LP, Rogers SD, Harkin DG. Effects of plasma proteins on the adhesion spreading polarization in suspension random motility and chemotaxis of neutrophil leukocytes on polycarbonate filtration membrane. *Eur J Cell Biol* 1990;53:27–34.

- [27] Roos FJ, Zimmermann A, Keller HU. Effect of phorbol myristate acetate and the chemotactic peptide fNLPNTL on shape and movement of human neutrophils. *J Cell Sci* 1987;88:399–406.
- [28] Keller HU, Zimmermann A, Cottier H (eds). Cell shape, movement and chemokinesis, vol. 66. Oxford: Pergamon, 1987.
- [29] Davis BH, Walter RJ, Pearson CB, Becker EL, Oliver JM. Membrane activity and topography of f-Met-Leu-Phe-treated polymorphonuclear leukocytes. *Am J Pathol* 1982;108:206–16.
- [30] Benton L, Purohit U, Khan M, Greco R. The biologic role of B2 integrins in the host response to expanded polytetrafluoroethylene. *J Surg Res* 1996;64:116–9.
- [31] Wright SD, Weitz JI, Huang AJ, Levin SM, Silverstein SC, Loike JD. Complement receptor type three (CD11b/CD18) of human polymorphonuclear leukocytes recognizes fibrinogen. *Proc Natl Acad Sci USA* 1988;85:7734.
- [32] Altieri D, Bader R, Mannucci P, Edgington T. Oligospecificity of the cellular adhesion receptor Mac-1 encompasses an inducible recognition specificity for fibrinogen. *J Cell Biol* 1988;107:1893–900.
- [33] Gustafson E, Lukasiewicz H, Wachtfogel Y, Norton K, Schmaier A, Niewiarowski S, Colman R. High molecular weight kininogen inhibits fibrinogen binding to cytoadhesins of neutrophils and platelets. *J Cell Biol* 1989;109:377–87.
- [34] Altieri D, Agbanyo F, Plescia J, Ginberg M, Edgington T, Plow E. A unique recognition site mediates the interaction of fibrinogen with the leukocyte integrin Mac-1 (CD11b/CD18). *J Biol Chem* 1990;265:12119–22.
- [35] Cooper J, Lo S, Malik A. Fibrin is a determinant of neutrophil sequestration in the lung. *Circul Res* 1988;63:735–41.
- [36] Weitz JI, Huang AJ, Landman SL, Nicholson SC, Silverstein SC. Elastase-mediated fibrinogenolysis by chemoattractant-stimulated neutrophils occurs in the presence of physiologic concentrations of antiproteinases. *J Exp Med* 1987;166:1836–50.
- [37] Higazi AA, Barghouti II, Ayesh SK, Mayer M, Matzner Y. Inhibition of neutrophil activation by fibrinogen. *Inflammation* 1994;18:525–35.
- [38] Loike J, Cao L, Silberstein S. The American society of cell biology. Washington DC, 1995.
- [39] Naziruddin BBFD, Tucker J, Mohanakumar T. Evidence for cross-regulation of Fc γ RII (CD32) expressed on polymorphonuclear neutrophils. *J Immunol* 1992;149:3702–9.
- [40] Graham IL, Lefkowitz JB, Anderson DC, Brown EJ. Immune complex-stimulated LTB $_4$ production is dependent on β 2 integrins. *J Cell Biol* 1993;120.
- [41] Nimeri G, Nilsson U, Lassen B, Goelander CG, Elwing H. Adsorption of fibrinogen and some other proteins from blood plasma at a variety of solid surfaces. *J Biomater Sci Polym Ed* 1994;6:573–83.
- [42] Ofek I, Sharon N. Lectinophagocytosis: a molecular mechanism of recognition between cell surface sugars and lectins in the phagocytosis of bacteria. *Infect Immunol* 1988;56:539–47.
- [43] Mukherjee G, Quinn MT, Linner JG, Jesaitis AJ. Remodeling of the plasma membrane after stimulation of neutrophils with f-Met-Leu-Phe and dihydrocytochalasin B: identification of membrane subdomains containing NADPH oxidase activity. *J Leuk Biol* 1994;55:685–94.
- [44] Harbecke O, Liu L, Karlsson A, Dahlgren C. Desensitization of the fMLP-induced NADPH-oxidase response in human neutrophils is lacking in okadaic acid-treated cells. *J Leuk Biol* 1997;61:753–8.
- [45] Rabinovitch M, Manejias RE, Nussenzweig V. Selective phagocytic paralysis induced by immobilized immune complexes. *J Exp Med* 1975;142:827–38.
- [46] Targowski SP, Niemialtowski M. Appearance of Fc receptors on polymorphonuclear leukocytes after migration and their role in phagocytosis. *Infect Immunol* 1986;52:798–802.
- [47] Gallin YI. Neutrophil specific granules and the inflammatory response. *Clin Res* 1984;32:320–8.
- [48] Bainton D. Sequential degranulation of the two types of polymorphonuclear leukocyte granules during phagocytosis of microorganisms. *J Cell Biol* 1983;58:249–54.